Abstract for International Conference on Advances in Product Metallurgy of Long and Forged Products
July 12-15 2015, Vail, CO

Modeling and Simulation of Hot Rolling using Nonlinear Material Models

X. Wang and K. Chandrashekhara

Department of Mechanical and Aerospace Engineering

S. A. Rummel, S. Lekakh, D. C. Van Aken and R. J. O'Malley

Department of Materials Science and Engineering
Missouri University of Science and Technology, Rolla, MO 65409

Keywords: hot rolling, round bar, mass flow, finite element, constitutive material model, strain rate

ABSTRACT

A Johnson-Cook material model was implemented in a commercial finite element code to simulate a two-stand thermo-mechanical tandem hot rolling process of a round bar. The finite element model incorporates experimental data obtained from Gleeble tests performed over a range of strain rates and temperatures. The critical parameters are monitored in the cross-section during two pairs of consecutive passes with bar cross section changing from round to oval and oval to round through each roll pair. Strain and strain rate distribution at each pass are determined for round bar. Equivalent plastic strain and plastic strain in each direction are compared with each other. Strain histories of different region on cross section are studied. Strain rate distribution on contact region is investigated. Results show specific distribution and history for strain and strain rate during round bar hot rolling process.

INTRODUCTION

Hot rolling is one of the most important deformation processes in steel manufacturing. In round steel bar hot rolling process, billets go through several roll passes with different roll gaps, roll shapes and roll speed. With specific rolling parameters, the resulting steel product may attain expected microstructure and mechanical properties, such as increased strength and improved ductility. Proper design of the hot rolling process is essential to continuous enhancing steel quality and productivity. Unlike a strip hot rolling process, a round bar has a more complicated stress and strain status during hot rolling. The steel bar is compressed from different directions at each roll pass, and the contact region is a cambered surface with non-uniform compressive force. Thus it is important to study mechanical parameters during hot rolling process.

Finite element analysis is an effective way to simulate the steel hot rolling process. Kim [1] provided a finite element simulation on non-isothermal hot rolling analysis, showing temperature gradients during the rolling process. Duan and Sheppard [2] proposed finite element model to simulate thermo-mechanical properties of aluminum alloy during a hot rolling process. Ding [3] developed numerical simulation for microstructure evolution and showed temperature had a more significant effect on recrystallization than roll speed. Mei [4] developed a finite element model to simulate strip temperature during hot rolling and Benasciutti [5] provided a finite element model to predict product thermal stresses during hot rolling. However, there has been very little published on simulations of round bar hot rolling and mechanical properties, which is essential to round bar fabrication.

Various material models have been developed to describe mass flow behavior during hot rolling process and the Johnson-Cook model [6] is a widely used phenomenological constitutive model which considers effects of strain hardening, strain rate hardening and temperature softening independently. This model is simple and easily implemented. Other models, such as the Zerilli–Armstrong model [7] is based on dislocation mechanisms, and construct different material models for BCC and FCC structures. The Shida model [8] provides an empirical constitutive model considering effect of carbon, strain, strain rate and temperature on plain carbon steels.

In the current work presented here, a three-dimensional nonlinear finite element model has been developed for hot rolling process. A Johnson-Cook material model was implemented in the simulation. Two continuous pairs of rollers were developed as being perfectly rigid and the round bar was modeled as being plastically deformable. The rolling process considered an intial round bar that was compressed by two consecutive rolling stands with sets of rollers in perpendicular to each other.

Strain distributions on cross section were detected after each stand and a detailed study of plastic strain was performed by plotting strain throughout the steel bar cross-section. Also, plastic strain in different directions were shown and compared. Strain history during multi-pass rolling process was studied and strain development on specific regions was shown. Strain rate on contact regions was also studied and specific strain rate distributions were plotted.

EXPERIMENTAL AND SIMULATION PROCEDURES

Material model

Steel grade 15V38 (C 0.38%, Mn 1.3%, Si 0.57%, Cr 0.13%, V 0.08%, Al 0.018%) was used to develop the materials model for this study. Specimens (15 mm length and 10 mm diameter) for compression tests were machined from continuously cast round bar and after rough hot rolling process. To investigate the effect of temperature and strain rate on flow stress, hot compression tests were conducted at four temperatures (1000°C, 1100°C, 1200°C and 1300°C) and five strain rates ($0.01s^{-1}$, $1s^{-1}$, $5s^{-1}$, $15s^{-1}$ and $30s^{-1}$). 20 combinations of temperature and strain rate were planned for hot compression tests. Three trials were performed for each combination. Before hot compression testing, the samples were heated up to 1300°C with a heating rate of 260°C/min, held for 3 min and cooled to the desired test temperature. Hot compression tests were performed using Gleeble thermo-mechanical machine [9] at selected constant temperature and constant strain rate.

Constitutive material model was needed to describe metal mass flow behavior during hot rolling process. Among constitutive material models, Johnson-Cook model has been widely used and has successfully described material mass flow behavior during steel hot forming process [10]. The form of Johnson-Cook model used in this study is presented in Eq. 1

$$\sigma = (A + B\varepsilon^{n})(1 + C\ln\dot{\varepsilon}^{*})(1 - T^{*m}) \tag{1}$$

where σ is equivalent flow stress, ε is equivalent plastic strain, $\dot{\varepsilon}^{*}$ is dimensionless strain rate which is $\dot{\varepsilon}^{*} = \dot{\varepsilon}/\dot{\varepsilon}_{0}$, $\dot{\varepsilon}$ is strain rate and $\dot{\varepsilon}_{0}$ is reference strain rate, T^{*} is homologous temperature which is $T^{*} = (T - T_{r})/(T_{m} - T_{r})$, T_{r} is reference temperature and T_{m} is metal melting temperature.

Constants, A, B, C, m and n, were calculated based on stress-strain data obtained from Gleeble hot compression tests. Twenty stress-strain curves were acquired under four temperatures and five strain rates. Stress-strain curves under strain rate 1 s^{-1} are shown in Figure 1.

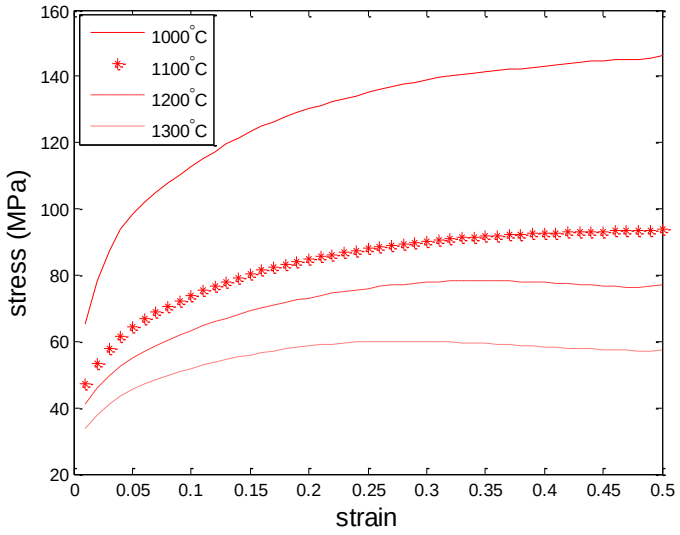

Figure 1. Stress-strain curves of 15V38 under strain rate 1 s^{-1}

A non-linear regression method was used to determine constants of Johnson-Cook model. Each set of constants was represented by one individual X. Fitness function (Eq. 2) of the regression was to minimize the sum of square error between experimental data and prediction of Johnson-Cook model.

$$\min f(x) = min\sum_{i=1}^{N}(\sigma_{i}^{exp} - \sigma_{i}^{JC}(X))^{2} \tag{2}$$
$$X = [A, B, n, C, m]$$

where N is number of experimental data points, σ_{i}^{exp} is experimental stress value at data point i, and $\sigma_{i}^{JC}(X)$ is Johnson-Cook model prediction based on constant set X at data point i. Constants determined for the 15V38 steel grade are shown in Table 1 and represents the Johnson-Cook material model implemented in the finite element models [11].

Table 1. Johnson-Cook constants of steel grade 15V38

	A	B	C	n	m
15V38	75.0	127	0.124	0.248	1.07

Finite element model

A nonlinear three-dimensional finite element model was developed to study a round bar hot rolling process. Formulation of three-dimensional dynamic analysis can be expressed in Eq. 3.

$$[M^e]\{\ddot{\Delta}^e\} + [K^e]\{\Delta^e\} = \{F^e\} \tag{3}$$

where $[M^e]$ and $[K^e]$ are mass matrix and the stiffness matrix respectively. $\{\Delta^e\}$ and $\{\ddot{\Delta}^e\}$ are displacement and acceleration respectively. $\{F^e\}$ is loading vector. The commercial software ABAQUS 6.10 Dynamic-Explicit solver was used to build finite element models. An explicit central-difference method was used for time integration:

$$\{\ddot{\Delta}^e\}_{(i)} = [M^e]^{-1}(\{F^e\}_{(i)} - \{I^e\}_{(i)}) \tag{4}$$

$$\{\dot{\Delta}^e\}_{(i+1/2)} = \{\dot{\Delta}^e\}_{(i-1/2)} + \frac{\Delta t_{i+1}+\Delta t_i}{2}\{\ddot{\Delta}^e\}_{(i)} \tag{5}$$

$$\{\Delta^e\}_{(i+1)} = \{\Delta^e\}_{(i)} + \Delta t_{(i+1)}\{\dot{\Delta}^e\}_{(i+1/2)} \tag{6}$$

where $\{I^e\}_{(i)}$ means internal force vector and subscript i represents increment step number. A three-dimensional isotropic round bar model was built with a diameter of 0.235m and a length of 4m. Two consecutive pairs of rollers (stand 1 and stand 2) were modeled as 3D rigid bodies and are shown in Figure 2. First pair of roller stand 1 was designed to compress steel bar from round to oval and second pair of roller stand 2 compressed steel bar from oval to round. Element C3D8RT was used to mesh the round bar. Element R3D4 was used to mesh the rigid roller. Johnson-Cook material models were implemented in finite element model. The initial temperature for round bar was 1100° C. Roller initial temperature was 150° C. Table 2 listed rolling process parameters. Specific mass flow parameters were detected during simulation process.

Figure 2. Modeling of round bar hot rolling process

Table 2. Parameter of rolling process

	Roller speed (rpm)	Roll gap (mm)	Pass depth (mm)
Stand 1	5.75	33.1	60.3
Stand 2	7.17	26.5	79.4

RESULT AND DISCUSSION

The finite element model was verified by comparing rolling torque with experimental data of stand 1. Average rolling torque of experimental data from Gerdau on stand 1 was 537 kN·m. Variations in rolling torque during hot deformation process

obtained from finite element simulation was depicted in Figure 3. During beginning of simulated hot rolling process, round bar was entering stand gap. As expected there is a sharp increase of torque in simulation results as the round bar entered the rolls. As rolling progressed, the simulated torque value stabilized to a value close to that reported for the experimentally reported torque [12].

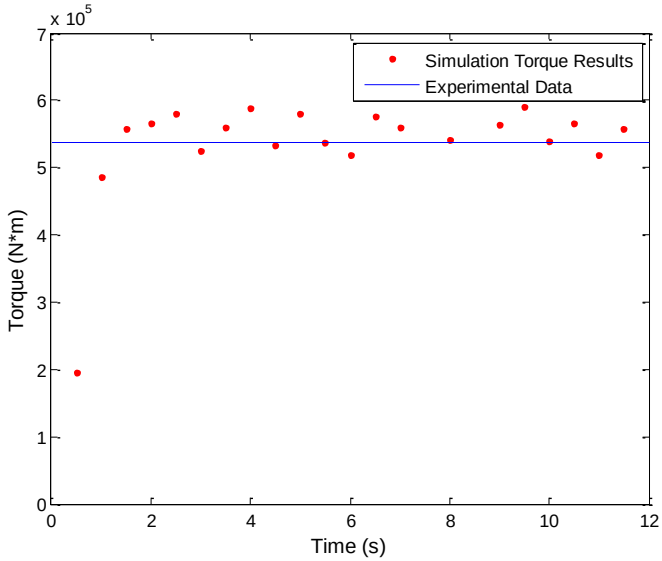

Figure 3. Stand 1 torque comparison of experimentally measured and simulated results

Plastic strain

Plastic strain distribution is important in hot rolling process, since microstructural refinement by recrystallization is dependent upon a critical strain. In addition, both pore closure and potential cracking are strongly dependent upon the maximum strain. Plastic strain distributions attained through finite element simulation include equivalent plastic strain and plastic strain in three different directions (see Figure 4).

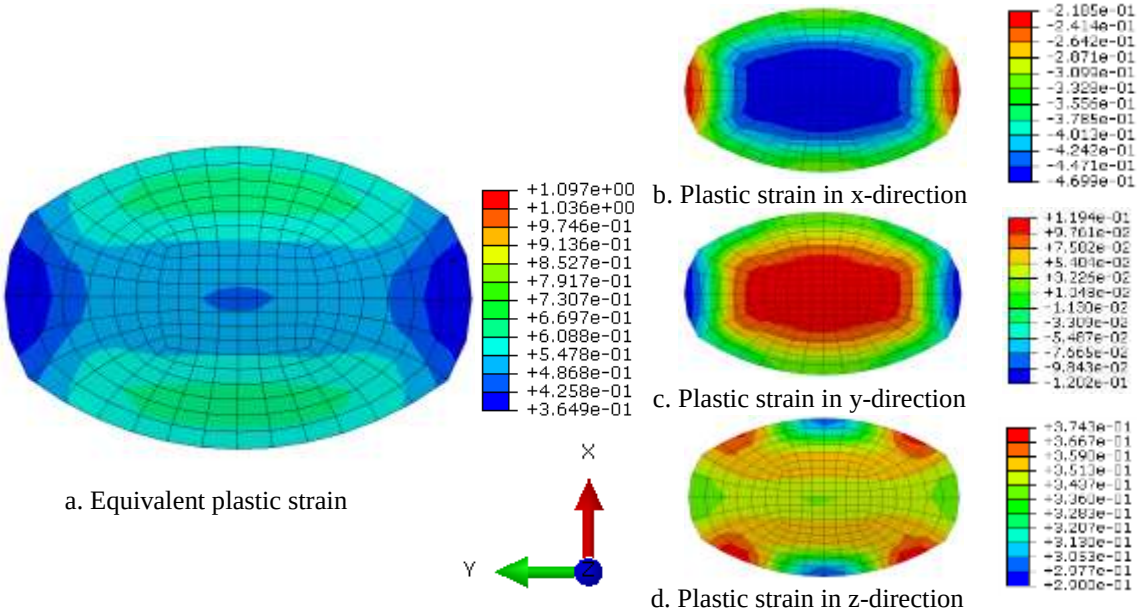

a. Equivalent plastic strain

Figure 4. Plastic strain distributions of 15V38 steel bar after stand 1

The equivalent plastic strain describes the strain status of the material being deformed and is calculated using Eq. 7.

$$\varepsilon_{eq} = \varepsilon_0^{pl} + \int_0^t \dot{\varepsilon}^{pl}\, dt \tag{7}$$

where ε_0^{pl} is initial equivalent plastic strain and $\dot{\varepsilon}^{pl}$ is equivalent strain rate. The equivalent plastic strain after roll pass 1 is

shown in Figure 4a. During stand 1, the round bar was compressed in the x-direction. Top and bottom areas in plot showed larger equivalent plastic strain status than internal and side areas. Minimal strain was evident on the two sides. Specific strain components of the strain tensor can also be displayed for the three normal strains. In the x-direction (Figure 4b), the maximum compressive plastic strain was at the bar center and the plastic strain decreased continuously to the bar surface. The smallest plastic strain in x-direction happened on the bar sides, which were not contacted by the rolls. All strains were compressive in nature. Plastic strain in the y-direction was a mixture of tension at the bar center and compression on the outer surfaces (see Figure 4c). Because of the large compressive deformation in the x-direction, the mass flowed towards the outside in the y-direction. During this rolling process, the roll surface held mass in the y-direction while the central portion of the bar flowed into the roll gap region, causing y-direction compression at the surfaces in the roll gap area. The free surfaces in the roll gap region produced lower compressive strains in the y-direction than in the x direction. In the z-direction (Figure 4d), the steel bar was elongated parallel to the rolling direction four regions shown as red in the figure had slightly larger plastic strain, which was caused by smaller frictional forces between the roll and the bar. Plastic strain in z-direction, generally, had similar value around 0.33.

A more detailed study of the plastic strain distributions was conducted and the plastic strain of surface nodes on the cross section was detected. Strain values were depicted along clockwise direction, shown in Figure 5. At angle ranges of 50°-150° and 220°-320°, plastic strain in x-direction had large value, while there were small strain values in y-direction and z-direction. Plastic strain curve in x-direction was almost opposite comparing to that in y-direction.

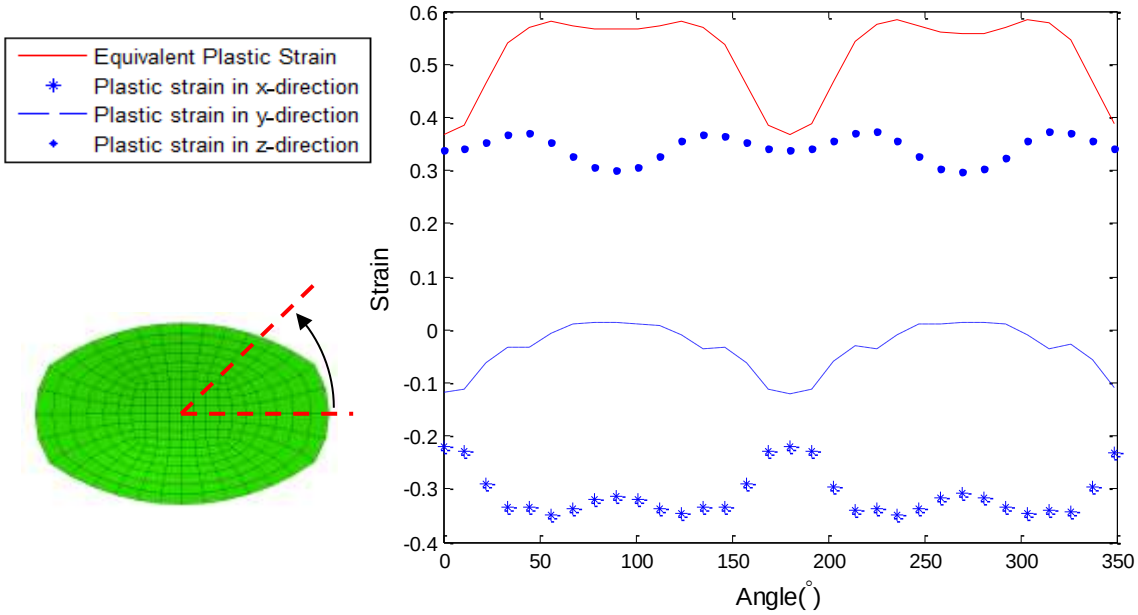

Figure 5. Plastic strain distributions along surface after stand 1

Plastic strain along horizontal diameter on cross section was also plotted (see Figure 6). From surface to internal area, plastic strain in x-direction inceased, while plastic strain in y-direction decreased and plastic strain in z-direction maintained a constant value.

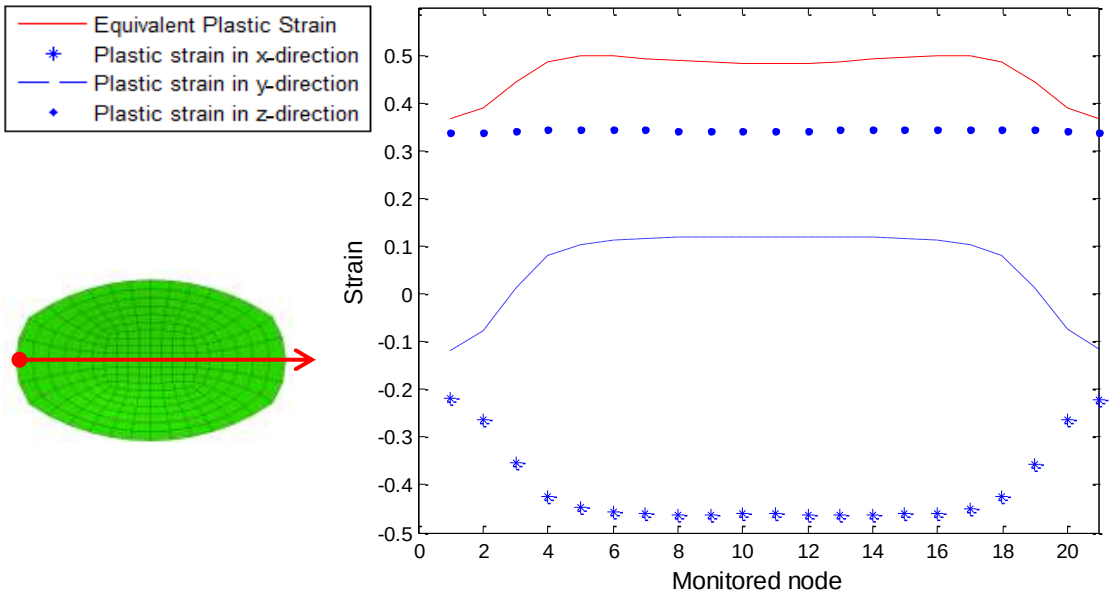

Figure 6. Plastic strain distribution of horizontal nodes after stand 1

Accumulated strains are shown in Figure 7 for the deformed bar after roll stand 2 and these strains represent the contributions from both roll stands 1 and 2. The maximum equivalent plastic strain was tensile and occurred at four red regions in Figure 7a. In the x-direction, the maximum plastic strain was compressive and located in two dark blue regions (Figure 7b), which were intermediate regions located between the bar center and the surface. Accumulated strains in the y-direction were also compressive with four regions (blue in Figure 7c) showing maximum compressive strains. Tensile strains were observed in the z-direction and plastic strain reached maximum value in red regions.

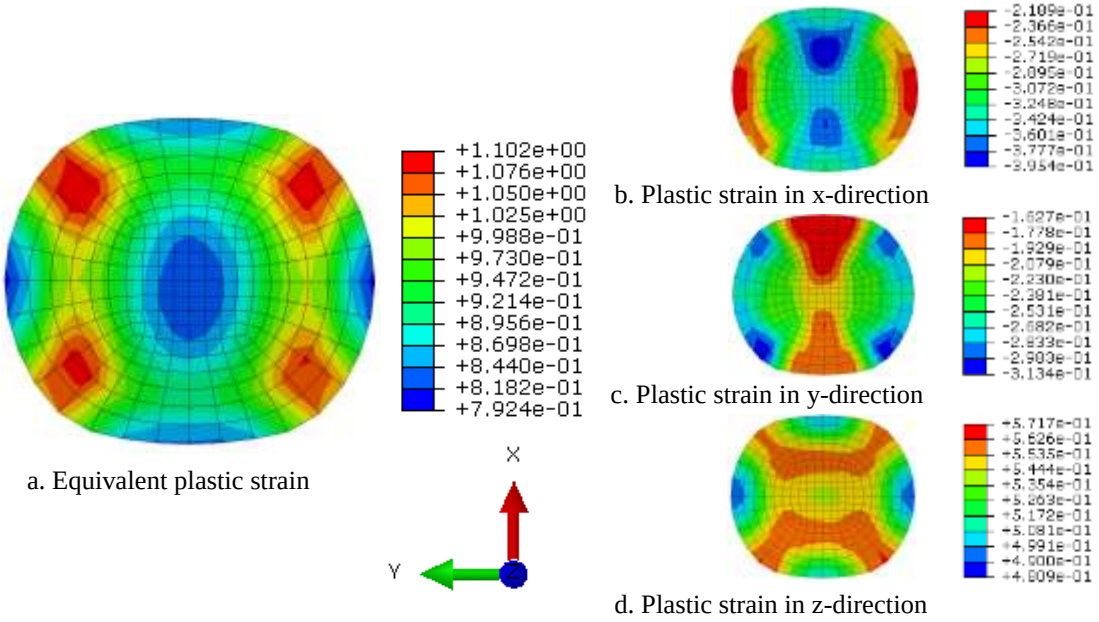

a. Equivalent plastic strain

b. Plastic strain in x-direction

c. Plastic strain in y-direction

d. Plastic strain in z-direction

Figure 7. Equivalent plastic strain distribution of bar after stand 2

Maximum plastic strains after each roll stand are shown in Table 3. After rolled by stand 1, steel bar achieved largest value in x-direction, while it was in z-direction after bar rolled by stand 2. These results can be explained by considering the change in roll orientation with each stand, which caused compression and tension on same region of the bar. At roll stand 1, the steel bar was compressed in the x-direction, causing compression in x-direction and partial tension in y-direction. However, after stand 2, steel bar was compressed in y-direction, causing a compressive relaxation in the x-direction and a tension relaxation in the y-direction. The strain in the z-direction was always tension and produced accumulated plastic strain and bar elongation.

Talbe 3. Maximum plastic strain value after each stand

	Maximum plastic strain			
	Equivalent plastic strain	x-direction	y-direction	z-direction
Stand 1	0.6	-0.47	+0.12/-0.12	+0.37
Stand 2 (accumulated)	1.1	-0.39	-0.31	+0.57

These calculations show that strain history is important for round bar hot rolling processes. Plastic strain developments in x-direction and y-direction were detected at specific nodes and plotted in Figure 8. In the x-direction, all of these five detected nodes were compressed after roll stand 1 at time 0-2s and shown by red lines. When the steel bar was rolled at stand 2, the plastic strain at these same nodes were all decreased by means of added tension strain Similarly in y-direction, expect point 5, detected nodes underwent tension in stand 1 and compression in stand 2.

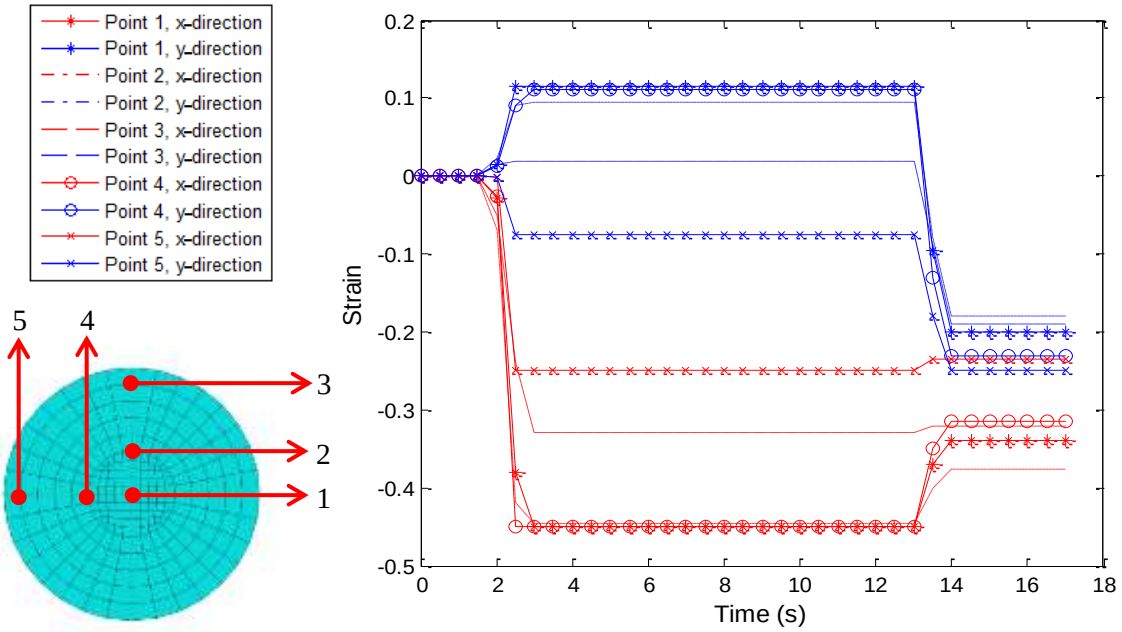

Figure 8. Plastic strain development of detected nodes

Strain rate

Strain rate was also studied in the current work. During hot rolling process, strain rate varied in a large range and its value directly affected steel mechanical property according to the Johnson Cook model. Strain rates of contact regions were detected parallel to the rolling direction. At rolling stand 1, ten nodes were selected along contact surface of steel bar (Figure 9). There were significant variation of strain rate in x-direction and z-direction, while strain rate in y-direction was very small. Along detected nodes, both x-direction and z-direction strain rates increased, reached maximum value of ±0.8 s^{-1} around node 3 and 4, and then decreased to 0.1 s^{-1} at node 6. Next, strain rate slightly increase and then decreased at region of node 8, 9 and 10. When the steel bar enters the rolling gap, bar speed is increased by rollers until neutral point. After neutral point, bar speed was deceased by roller.

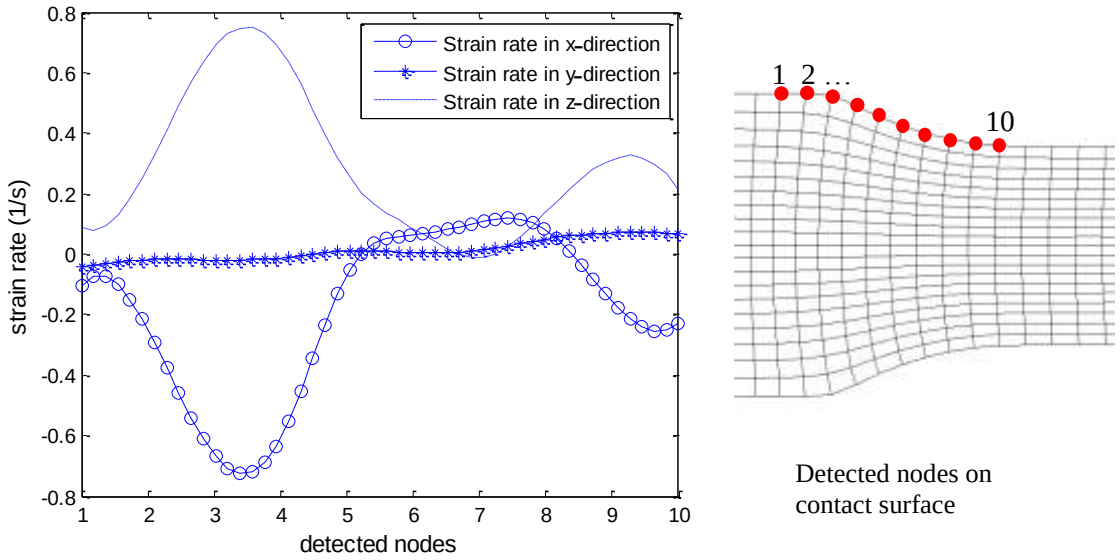

Figure 9. Strain rate distribution on contact region of stand 1

Similar situation happened at roll stand 2. Since contact region of stand 2 was shorter than that of stand 1, there were nine nodes detected. Corresponding strain rates were plotted in Figure 11. At roll stand 2, the steel bar was compressed in y-direction and therefore the strain rate in the x-direction was small (give value). In the y-direction, the strain rate increased to maximum value of (give value) around node 3 and then decreased to minimum value of (give value) at node 5. After that the strain rate increased again and then reduced. A similar strain rate response as observed for the y-direction was also observed in the z-direction.

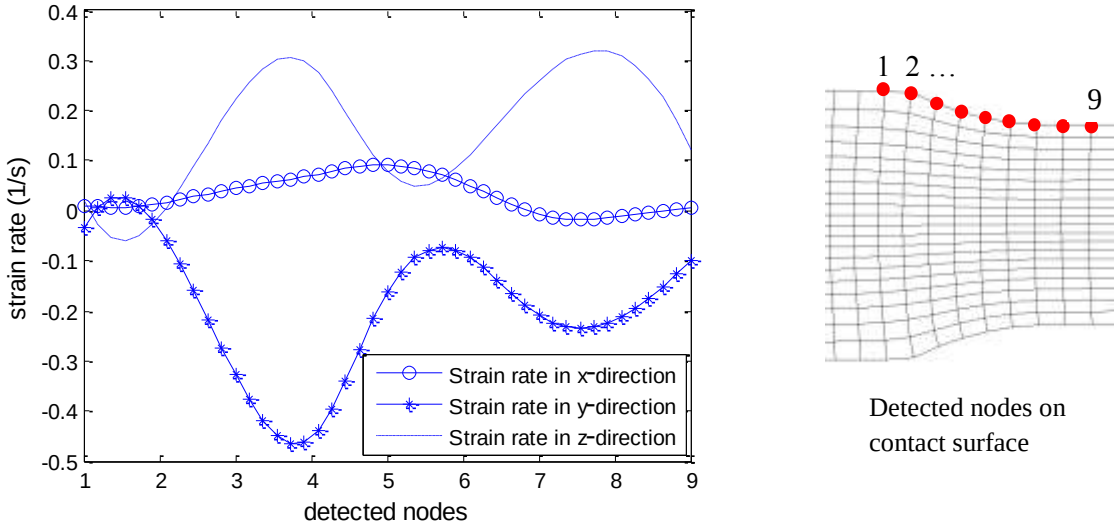

Figure 10. Strain rate distribution on contact region of stand 2

CONCLUSION

A three-dimensional nonlinear finite element model was developed for round bar hot rolling process. Two rolling stands were modeled, one was a vertical compression pass and the second was a horizontal compression pass. A Johnson-Cook constitutive material model was implemented in a finite element analysis to predict mass flow behavior. The material model was sensitive to strain rate and temperature. Nonlinear regression method was used to determine material model constants. Strain and strain rate were studied and the following conclusions could be drawn:

1. Plastic strain distributions after roll stand 1 had compressive strains in the x-direction and z-direction, while in the y-direction the material mainly underwent tension. The maximum strains in x-direction and y-direction were in internal regions, while maximum strain in z-direction occurred at the surface.

2. After roll stand 2, accumulated strain distribution patterns changed significantly in both x-direction and y-direction. Maximum equivalent plastic strain was shown in four subsurface regions, nearly ±45°/±135° from horizontal line. Strain in the z-direction was an accumulation of tensile strains from each roll pass.
3. During the hot rolling process, material underwent both compression and tension. The alternate deformation could increase crack generation. Especially in y-direction, variation of strain exceeded 30 percent, from tension to compression.
4. Strain rate distributions in contact region showed a two-bump curve. It showed strain rate increased to maximum value and then decreased to a stable status. Next strain rate increased and decreased again.

ACKNOWLEDGEMENTS

This work was supported by the Peaslee Steel Manufacturing Research Center at Missouri University of Science and Technology. The authors would like to thank Geary W. Ridenour, Mike Kolljeski and Ross Wilkinson from Gerdau-Fort Smith for their practical input. Finally, Todd Link from US Steel Corporation and Rafael Pizarro Sanz from Gerdau Aceros Especiales Europa for Gleeble testing.

REFERENCES

[1] S. Kim and Y. Im, "Three-dimensional finite element analysis of non-isothermal shape rolling," *Journal of Materials Processing Technology*, vol. 127, pp. 57–63, 2002.

[2] X. Duan and T. Sheppard, "Three dimensional thermal mechanical coupled simulation during hot rolling of aluminium alloy 3003," *International Journal of Mechanical Sciences*, vol. 44, pp. 2155–2172, 2002.

[3] H. Ding, K. Hirai, T. Homma, and S. Kamado, "Numerical simulation for microstructure evolution in AM50 Mg alloy during hot rolling," *Computational Materials Science*, vol. 47, pp. 919–925, 2010.

[4] R. Mei, C. Li, X. Liu, and B. Han, "Analysis of strip temperature in hot rolling process by finite element method," *Journal of Iron and Steel Research International*, vol. 17, pp. 17–21, 2010.

[5] D. Benasciutti, E. Brusa, and G. Bazzaro, "Finite elements prediction of thermal stresses in work roll of hot rolling mills," *Procedia Engineering*, vol. 2, pp. 707–716, 2010.

[6] G. R. Johnson and W. H. Cook, "A constitutive model and data for metals subjected to large strains, high strain rates and high temperatures," *7th International Symposium on Ballistics*, vol. 21, pp. 541–547, 1983.

[7] F. J. Zerilli and R. W. Armstrong, "Dislocation-mechanics-based constitutive relations for material dynamics calculations," *Journal of Applied Physics*, vol. 61, pp. 1816–1825, 1987.

[8] S. Shida, "Empirical formula of flow stress of carbon steels—resistance to deformation of carbon steels at elevated temperature," *Journal of the Japan Society for Technology of Plasticity*, vol. 10, pp. 610–617, 1969.

[9] Y. Sun, W. D. Zeng, Y. Q. Zhao, Y. L. Qi, X. Ma, and Y. F. Han, "Development of constitutive relationship model of Ti600 alloy using artificial neural network," *Computational Materials Science*, vol. 48, pp. 686–691, 2010.

[10] Y. Lin and X. Chen, "A critical review of experimental results and constitutive descriptions for metals and alloys in hot working," *Materials & Design*, vol. 32, pp. 1733–1759, 2011.

[11] S. Rummel, D. Van Aken, R. O'Malley, X. Wang, and K. Chandrashekhara, "High Strain Rate Hot Deformation of Steels: Measurement and Simulation," in *AIST Long and Forged Products Symposium*, 2015.

[12] Gerdau, "Power and speed study," 2006.